ISSN 1028-334X, Doklady Earth Sciences, 2007, Vol. 415, No. 5, pp. 744–750. © Pleiades Publishing, Ltd., 2007.
Original Russian Text © A.I. Kiselev, V.V. Yarmolyuk, A.V. Nikiforov, K.N. Egorov, 2007, published in Doklady Akademii Nauk, 2007, Vol. 414, No. 6, pp. 798–804.

GEOCHEMISTRY

Composition and Sources of Devonian Volcanism in the Vilyui Rift

A. I. Kiselev[a], Corresponding Member of the RAS V. V. Yarmolyuk[b], A. V. Nikiforov[b], and K. N. Egorov[a]

Received December 12, 2006

DOI: 10.1134/S1028334X07050194

Riftogenic processes were widespread in the Middle Paleozoic history of the Earth. They produced several rift systems and regions in the Siberian Craton. The Vilyui rift zone (VRZ) or paleorift (~800 km long and 450 km wide [1, 2]) occupies a special place among them. The VRZ represents a blind offshoot of a three-member rift system. The other two offshoots of this system split the Siberian paleocontinent in the Middle Paleozoic and defined its present-day boundary [3]. The paleorift has a complex structure with dike belts extending along its walls. The internal structure of the paleorift represents a system of longitudinal depressions separated by uplifts. The depressions are filled with Upper Devonian–Lower Carboniferous sedimentary, volcanic, and volcanosedimentary rocks. The northwestern wall of the rift incorporates the Vilyui–Markha mafic dike belt with the Mirnin and Nakyn diamondiferous kimberlite fields (Fig. 1). In terms of some essential parameters, such as the huge area ($n \cdot 10^5$ km^2) of volcanic fields, the presence of large dike belts and thick dikes, and the development of thick sills and kimberlites in the riftogenic complexes, the VRZ matches superplume-related provinces [4]. Therefore, Devonian rifting and associate magmatism in the eastern Siberian Craton can be attributed to the influence of a large plume on the continental lithosphere [5]. However, the compositional parameters of the plume could not be estimated until recently because of the absence of information on the geochemical and isotopic characteristics of the volcanic rocks that make up the major volume of igneous rocks in the paleorift. Based on original Sr–Nd data and the ICP-MS determination of trace elements in volcanic rocks of the VRZ, first estimates of the composition and geochemical specifics of deep-seated mantle sources of magmatism responsible for rifting of the region are reported in the present paper.

OVERVIEW OF THE GEOLOGICAL SETTING

The stratigraphy, tectonics, and distribution of volcanosedimentary sequences in depressions of the VRZ are scrutinized in [1, 2]. Basalt sheets are developed both within rift depressions (intercalation with Devonian terrigenous and carbonate rocks) and beyond the depressions. The productivity of volcanism increases distinctly from southwest to northeast along the strike of the Vilyui rift. The total thickness of the volcanic-hosting terrigenous–carbonate sequences also shows a similar trend. Generally, volcanic sheets prevail in the lower sections of Devonian sequences. However, the volcanics also dominate at some upper levels, indicating the multistage manifestation of volcanism. Volcanosedimentary sequences are usually dislocated by numerous low-angle faults.

The initial (Middle Devonian [2]) stage of the VRZ evolution was marked by the appearance of a flat depression filled with carbonate–clayey sediments at the site of the future Vilyui syneclise. The second stage (first half of the Frasnian) promoted the formation of a large dome, which occupied a significant area of the syneclise, and the synchronous development of grabens and depressions. These processes were accompanied by large-scale effusions of basalt lavas that made up several sequences (or formations) of volcanic rocks. This stage was most likely also characterized by the emplacement of sheeted and crosscutting basic bodies that made up dike belts on offshoots of the rift. The final (terminal Frasnian–Famennian) stage was marked by a drastic reduction of the large-scale effusion of basalt lavas in the course of the intensification of contrasting tectonic movements in the rift. In the western part of the rift, this stage was characterized by the development of the amagmatic Kempendyai Depression (major rift valley) filled with sedimentary rocks (3–7 km thick) and several smaller depressions (Fig. 1). The Early Carbon-

[a] *Institute of the Earth's Crust, Siberian Division, Russian Academy of Sciences, ul. Lermontova 128, Irkutsk, 664033 Russia; e-mail: akiselev@crust.irk.ru*

[b] *Institute of Geology of Ore Deposits, Petrography, Mineralogy, and Geochemistry, Russian Academy of Sciences, Staromonetnyi per. 35, Moscow, 119017 Russia*

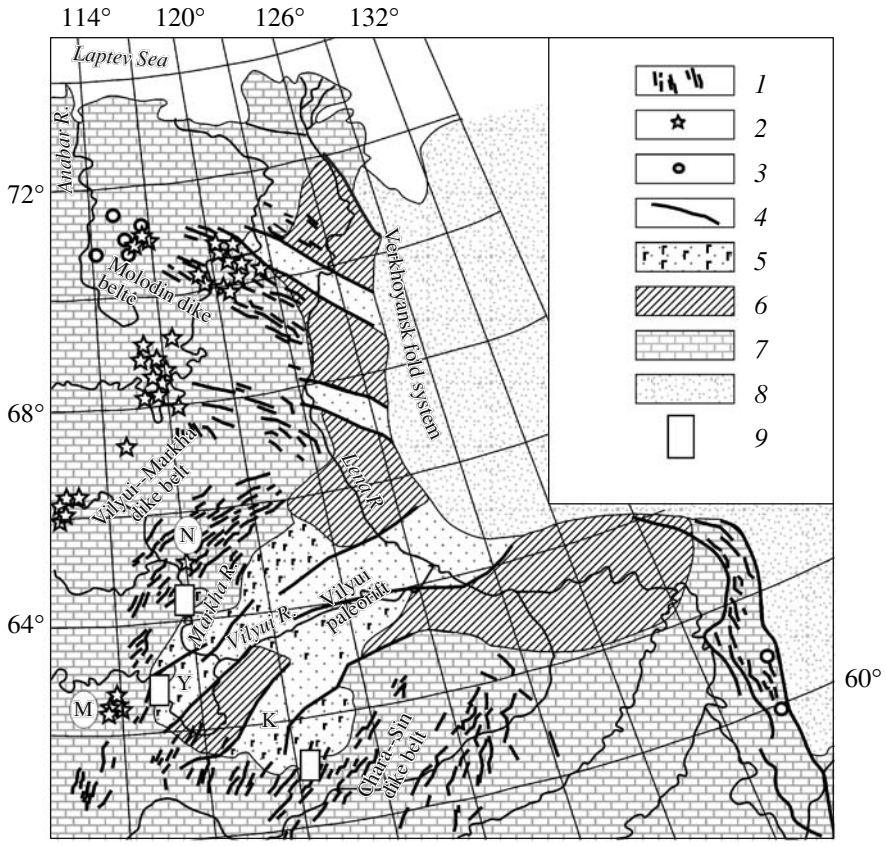

Fig. 1. Geological scheme of the Middle Paleozoic Vilyui rift system. (*1*) Basic dikes; (*2*) kimberlites; (*3*) massifs of alkaline ultramafic rocks and carbonatites; (*4*) faults; (*5*) effusive–sedimentary sequences of rift depressions; (*6*) relatively uplifted areas (relicts of paleodome); (*7*) Siberian Craton; (*8*) Verkhoyansk fold system; (*9*) areas of igneous rock sampling; depressions: (Y) Ygyatta, (K) Kempendyai; Kimberlite fields: (M) Mirnin, (N) Nakyn.

iferous history was marked by attenuation of tectonic displacements and volcanic activity. Processes of riftogenic gave way to the formation of the syneclise beginning in the Upper Paleozoic.

We investigated the isotope–geochemical characteristics of igneous rocks from the northwestern and southwestern areas of the VRZ (Fig. 1). The igneous rocks can be divided into two series corresponding to two lava sequences. The early series includes rocks of the Namana Formation confined to the Saran and Berezov depressions in the southwestern Vilyui rift. The late series is composed of basalts of the Appain Formation (Ygyatta Depression and Markha River Valley) and the Khaialakh Formation overlapping the Namana Formation in the southwestern Vilyui rift area. According to our opinion, the late series also includes pre-kimberlite dikes developed in the Vilyui–Markha dike belt at the northwestern framing of the rift system. The dikes are compositionally similar to basalts of the rock formations mentioned above. Thus, rocks of the late series characterize the magmatic stage manifested over the entire rift zone.

Volcanic rocks of the Namana Formation are represented by a differentiated series with composition varying from trachybasalts to trachyandesites. The total thickness is as much as 750 m, and the igneous rocks account for ~60–90% of the section [1]. The Namana Formation also includes trachybasalts, basaltic trachyandesites, and normal trachyandesites. Rocks of the series are characterized by the presence of dissemination of plagioclase, clinopyroxene, and hornblende (including overgrowths on pyroxene grains). Olivine is confined to basalts. Basaltic trachyandesites and trachyandesites include ore mineral, biotite, and apatite.

The Appain and Khaialakh formations are characterized by 20- to 60-m-thick sheets of more or less homogeneous basalts. They are separated by thin units of terrigenous and carbonate rocks. The thickness of these formations varies from 10*n* to 200 m. Their Late Devonian age is based on paleontological data. Volcanic rocks of the sequence are represented by tholeiitic and moderately alkaline porphyritic basalts with phenocrysts of olivine (replaced by bowlingite) and plagioclase. The matrix includes plagioclase, clinopyroxene, titanomagnetite, ilmenite, single biotite flakes associated with titanomagnetite, and occasional accessory apatite.

PETROGEOCHEMICAL AND ISOTOPE–GEOCHEMICAL CHARACTERISTICS OF IGNEOUS ROCKS

The table presents representative analyses of igneous rocks of the Vilyui paleorift. Basalts of the Appain and Khaialakh formations have similar petrochemical characteristics. They belong to the petrochemical series of tholeiitic and moderately alkaline rocks with the following contents of major oxides (wt %): SiO_2 46.5–50; TiO_2 1.7–2.6; Al_2O_3 14–16; MgO 5.5–8; $Na_2O + K_2O$ 2.2–3.3. In some plagiophyric basalts, the Al_2O_3 content increases to 19% and that of MgO decreases to 4%. In general, the TiO_2 content (1.8–2.5%) in basalts of the Appain and Khaialakh formations is similar to that in dolerites in the sill (probably coeval to effusives) of the Mirnin district. However, the TiO_2 content is much lower than that in younger (pre-kimberlitic) dolerite dikes (~3.33%) and rocks of the Namana Formation (2.4–3.3%). Relative to basalts of the Appain and Khaialakh formations with comparable SiO_2 contents, rocks of the Namana Formation are enriched in $K_2O + Na_2O$ (6.2–7.5%) and P_2O_5 (~1%), but they are depleted in CaO and MgO. Rocks of these formations also differ in terms of the parameter $Mg\# = Mg/(Mg + Fe^{2+})$. This parameter is 0.6–0.5 in the Appain and Khaialakh basalts and 0.35–0.23 in the Namana basalt. The contents of indicator compatible elements in these formations show the following variation range: Ni 150–40 and 25–10 ppm, respectively; Cr 380–45 and 23–8 ppm, respectively. Therefore, we believe that primary mantle melts were significantly differentiated owing to the fractionation of olivine and pyroxene and, probably, contamination with lithospheric material in the course of the exhumation of melts. The latter assumption is mainly based on the isotope data given below. The presence of porphyric segregations of olivine, clinopyroxene, plagioclase, and Ti–Fe oxides in lavas suggests that fractionation was related to crystallization of these minerals.

Regularities in the distribution of incompatible elements in igneous rocks of the Vilyui rift are shown as spidergrams (Fig. 2). The compositional spectra of basalts of the Appain and Khaialakh formations are similar and identical to those of moderately titaniferous (TiO_2 <3%) basic rocks of the Nakyn dike belt [6, 7] at the northwestern boundary of the VRZ. The concentrations of LREEs are lower (La/Yb 10–16) than in the OIB, probably due to the involvement of granite in the process of melting.

In contrast to basalts of the Appain and Khaialakh formations, rocks of the Namana Formation are generally enriched in incompatible elements, relative to the OIB [8] and high-Ti basic rocks of the Nakyn dike belt. The concentrations of the incompatible elements are maximal in trachyandesites, presumably due to fractionation of the primary melt. These igneous rocks are characterized by a higher degree of LREE fractionation (relative to the Appain basalt) and the consequent rise of the $(La/Sm)_N$ value from trachybasalts (4.0–4.5) to trachyandesites (5.6–6.1). At later stages of the melt evolution probably accompanied by an increase in the water content, the pyroxene–plagioclase fractionation gave way to amphibole–plagioclase (oxides and apatite) fractionation. This assumption is supported by the lower concentrations of Fe, Ti, and P in the trachyandesites than in the trachybasalts (table).

Not only tholeiitic and transitional basalts of the Appain and Khaialakh formations, but also rocks of the trachybasalt–trachyandesite series demonstrate surprisingly similar Nd and Sr isotopic compositions (table). In the $\varepsilon_{Nd}(1.8–2.2)$–$\varepsilon_{Sr}(4.6–7.7)$ diagram, data points of igneous rocks make up a compact cluster in the upper part of the mantle array, suggesting the involvement of a sufficiently uniform mantle source. Its composition was defined by combination of the moderately depleted PREMA-type mantle and the Sr-rich EM II-type mantle (Fig. 3). The relatively higher Sr isotope ratio (0.70581, $\varepsilon_{Sr} = 25.2$) in one basalt sample (K-159) of the Khaialakh Formation can be provoked by contamination with carbonate material. The isotopic compositions of igneous rocks are distinguished markedly from those of subvolcanic intrusions of the Markha dike belt by lower ε_{Nd} values and smaller variation ranges of ε_{Sr}. These discrepancies are caused by the following fact [6, 7]: the formation of melts involved the participation of subvolcanic intrusions of an enriched source (probably carbonate–evaporite material) characterized by high concentrations of LILE elements (K, Ba, and Sr) and relatively lower concentrations of REE and other elements.

Thus, igneous rocks of the Vilyui rift represent a part of the huge (600×1000 km) region of basaltic magmatism. The igneous rocks are confined to maximal extension zones (rift depressions and their nearest surroundings). The available isotope–geochemical data suggest a link between magmatism and plume activity. The geochemical specialization of igneous rocks was presumably governed by different degrees of melting in the source with a uniform isotopic composition. In terms of indicator ratios (Zr/Nb 4–14, La/Nb 0.6–1.6, Th/Nb >0.21, and Th/La <0.15), the source was similar to the enriched mantle source that controlled the formation of oceanic islands [9].

The earliest manifestation of basaltic magmatism is represented by a small area of trachybasalt–trachyandesite lavas of the Namana Formation in the southwestern part of the Vilyui rift. A mantle source with a considerable amount of the fluid component and alkali metals could participate in the formation of this area. The lavas are characterized by concentrations of incompatible elements 3–5 times higher relative to rocks of the Appain and Khaialakh formations. Therefore, we assume that the specific geochemistry of the lavas mentioned above was stipulated not only by the higher degree of melt fractionation, but also by the lower degree of melting.

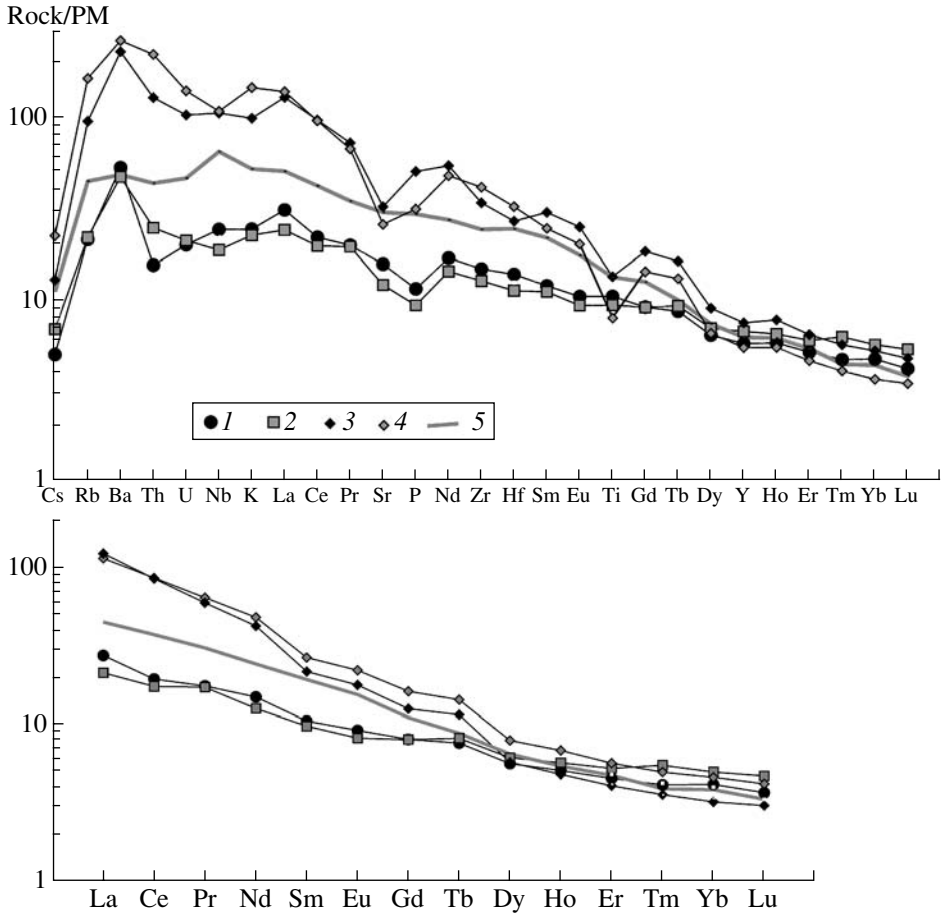

Fig. 2. Contents of PM-normalized incompatible and rare earth elements (according to [8]). (*1*) Basalts of the Appain Formation; (*2*) basalts of the Khaialakh Formation; (*3, 4*) trachybasalts and trachyandesites, respectively, of the Namana Formation; (*5*) OIB.

The later phase of basaltic magma generation was manifested as large-scale effusions of tholeiitic and moderately alkaline basalts (Appain and Khaialakh formations), as well as intrusions of dolerite sills and dikes at offshoots of the Vilyui rift. The relatively lower alkalinity of these igneous bodies could be related to the higher melting degree of mantle sources. The isotope–geochemical homogeneity of volcanic products reflects the homogeneity of magmatic sources beneath the entire rift system. In terms of the isotopic composition, intrusions of the Vilyui–Markha dike belt show some distinctions from the cognate igneous rocks, probably because of the contamination of the latter rocks with the carbonate–evaporate material.

The terminal stage of basalt magmatism has been established only in the Vilyui–Markha dike belt at the northwestern offshoot of the Vilyui rift. Here, Ti- and K-rich basic dikes intrude kimberlites of the Nyurba Pipe in some places [7]. These rocks could form during the cooling of the plume head, resulting in subsidence of the magma formation level and decrease in the melting degree of the mantle substrate.

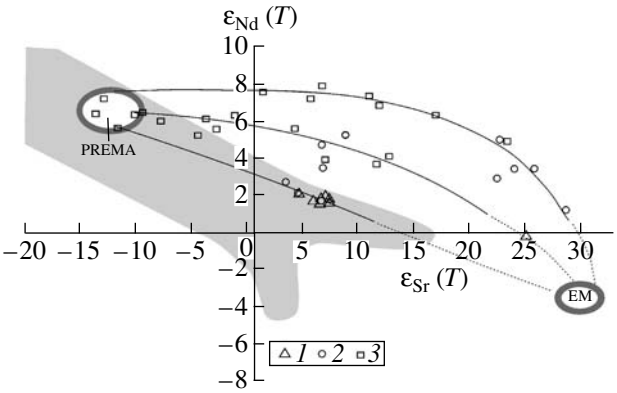

Fig. 3. ε_{Nd}–ε_{Sr} diagram for igneous rocks of the Vilyui paleorift. Mantle sources: (PREMA) moderately depleted mantle, (EM) mantle enriched in radiogenic Sr. The gray area shows the compositional field of mantle rocks (mantle array). Lines show mixing hyperbolas corresponding to different Sr/Nd values in sources. (*1*) Effusives of the Appain, Khaialakh, and Namana formations; (*2*) basic rocks of the northwestern offshoot of the Vilyui paleorift; (*3*) Middle Paleozoic basalts of the Altai–Sayan region [7].

Representative analyses of igneous rocks of the Vilyui rift

Component	Appain Formation				Khaialakh Formation		Namana Formation					
	427/2	420/54	420/32	418/5b	K-152	K-159	K-207	K-229	K-170	K-162	K-140	K-134
SiO_2	48.34	48.78	49.14	48.26	47.59	49.63	50.66	49.84	50.82	51.58	57.91	57.91
TiO_2	2.53	2.34	2.54	2.57	1.81	1.72	2.99	3.28	2.96	2.91	1.68	1.67
Al_2O_3	14.38	14.41	14.11	14.23	14.95	15.85	14.50	14.60	14.35	14.35	15.50	15.55
Fe_2O_3	12.02	12.49	12.13	12.06	1.91	4.55	11.13	8.25	9.31	6.86	6.98	6.93
FeO					11.42	6.32	2.21	4.71	4.01	5.63	2.00	1.54
MnO	0.15	0.16	0.14	0.13	0.18	0.18	0.13	0.16	0.11	0.18	0.05	0.08
MgO	5.78	6.08	5.83	6.64	7.70	6.16	2.78	3.01	3.25	3.35	1.52	1.44
CaO	10.20	10.26	10.10	9.59	10.37	10.90	5.83	6.59	6.05	6.12	2.79	3.45
Na_2O	2.37	2.16	2.44	2.32	2.31	2.20	3.99	3.82	3.84	3.86	4.44	4.57
K_2O	0.84	0.71	0.79	0.81	0.45	0.37	2.66	2.36	2.51	2.44	4.10	4
P_2O_5	0.28	0.26	0.28	0.29	0.17	0.16	1.10	1.11	1.10	1.08	0.66	0.66
L.O.I.	1.65	0.95	1.01	1.79	0.97	1.52	1.61	1.68	1.40	1.35	1.40	1.42
Total	98.54	98.60	99.86	100.03	100.19	99.98	100.04	99.89	100.27	100.26	99.71	99.93
$Mg^{\#}$	0.53	0.53	0.53	0.56	0.55	0.55	0.32	0.34	0.35	0.35	0.25	0.25
Sc	31.70	26.70	41.60	41.60	34.89	33.76	17.11	21.38	19.25	18.23	100.08	10.611
V	311.00	240.00	374.70	368.00	319.16	305.28	232.22	263.53	245.98	222.97	106.34	100.43
Cr	139.00	62.30	172.00	175.70	228.89	166.41	17.95	15.19	16.27	15.80	23.03	8.388
Co	37.30	39.90	46.00	48.10	53.46	40.66	28.49	29.72	32.94	29.20	16.41	17.755
Ni	44.80	42.40	74.90	75.90	127.72	74.45	19.08	22.10	18.93	18.75	10.85	8.533
Rb	18.20	13.80	19.30	21.00	12.05	5.88	55.24	53.61	57.10	56.57	108.90	105.95
Sr	356.00	318.00	380.70	397.00	197.09	332.68	715.63	745.62	715.41	718.86	545.86	588.19
Y	24.60	22.80	29.10	28.30	32.91	25.38	36.86	34.20	37.84	35.63	23.66	27.106
Zr	157.00	139.00	335.20	191.50	114.17	129.17	409.38	371.00	336.27	365.28	510.79	447.74
Nb	19.60	16.40	22.60	23.40	5.60	17.95	61.64	82.69	80.02	79.73	80.32	80.208
Cs	0.22	0.11			0.34	0.10	0.24	0.34	0.34	0.41	0.79	0.688
Ba	238.00	192.00	283.50	929.10	154.79	423.30	1474.04	1644.98	1696.92	1569.94	1935.74	1928.9
La	28.80	24.10	21.05	20.40	9.69	19.14	96.99	89.48	91.78	91.43	102.61	100.89
Ce	60.10	49.90	48.83	46.67	22.64	38.34	182.58	182.39	182.66	176.80	185.68	179.69

Table. (Contd.)

Component	Appain Formation				Khaialakh Formation		Namana Formation					
	427/2	420/54	420/32	418/5b	K-152	K-159	K-207	K-229	K-170	K-162	K-140	K-134
Pr	6.80	5.79	6.35	6.15	2.96	7.76	20.15	19.81	20.53	20.05	18.34	19.34
Nd	27.70	22.30	28.01	27.36	13.79	19.44	77.44	78.30	78.11	75.06	65.86	69.092
Sm	5.85	4.61	6.56	6.35	4.10	4.51	14.01	14.55	14.16	13.54	10.83	11.653
Eu	1.83	1.44	2.16	2.13	1.40	1.47	4.26	4.45	4.34	4.19	3.36	3.542
Gd	5.68	4.67	6.32	6.05	4.96	4.64	11.10	12.52	11.18	11.17	8.17	9.109
Tb	0.88	0.75	0.99	0.93	0.84	0.76	1.65	1.58	1.65	1.62	1.21	1.333
Dy	5.04	4.28	5.54	5.42	5.29	4.30	7.08	7.15	7.02	6.82	4.68	5.165
Ho	1.03	0.89	1.08	1.04	1.11	0.88	1.26	1.24	1.96	1.21	0.82	0.989
Er	2.68	2.32	2.94	2.72	3.16	2.30	3.34	3.08	3.38	3.20	2.19	2.332
Tm	0.38	0.32	0.46	0.43	0.55	0.39	0.46	0.44	0.47	0.46	0.31	0.33
Yb	2.24	1.90	2.71	2.29	3.11	2.30	2.78	2.73	2.66	2.58	1.74	1.865
Lu	0.30	0.25	0.40	0.36	0.48	0.34	0.39	0.39	0.38	0.39	0.27	0.279
Hf	3.95	3.35	8.24	4.64	2.76	3.06	8.34	8.67	7.45	7.89	10.97	9.653
Ta	1.12	0.98	1.48	1.52	0.27	0.76	2.32	3.31	2.75	2.86	3.14	4.663
Pb	0.38	0.05	2.46	2.02	4.07	5.20	11.00	10.02	10.29	9.77	24.44	20.454
Th	1.84	1.31	2.26	2.10	1.19	2.34	10.81	9.98	11.05	10.99	20.88	20.35
U	0.50	0.39	0.64	0.57	0.38	0.46	2.72	2.03	2.20	2.21	3.33	2.881
$^{87}Rb/^{86}Sr$	0.14	0.121	0.15	0.16	0.171	0.050	0.233	0.206	0.238	0.237	0.576	0.540
$^{87}Sr/^{86}Sr$	0.70530	0.70500	0.70537	0.70535	0.70540	0.70609	0.70586	0.70573	0.70589	0.70590	0.70773	0.70751
$^{87}Sr/^{86}Sr_{(T)}$	0.70450	0.70440	0.70454	0.70446	0.70445	0.70581	0.70456	0.70458	0.70457	0.70459	0.70453	0.70452
$\varepsilon_{Sr}(T)$	6.6	4.6	7.0	6.0	5.9	25.2	7.4	7.7	7.4	7.7	7	6.7
$^{147}Sm/^{144}Nd$	0.13731	0.13966			0.18043	0.14167	0.1010	0.10141	0.1010	0.1009	0.0226	0.09443
$^{147}Nd/^{144}Nd$	0.51257	0.51260			0.51269	0.51248	0.51245	0.51249	0.51249	0.51249	0.51247	0.51247
$\varepsilon_{Nd}(T)$	1.75	2.18			1.8	−0.3	1.8	1.9	1.8	1.8	1.9	1.9

Note: Sm–Nd and Rb–Sr isotopic determinations were made by A.V. Nikiforov in line with standard methods at the Institute of Geology of Ore Deposits, Petrography, Mineralogy, and Geochemistry, Moscow. The *T* value is adjusted for an age of 390 Ma. Ratios are calculated with an error of no more than 1% $^{87}Rb/^{86}Sr$, 0.01% for $^{87}Sr/^{86}Sr$, 0.5% for $^{147}Sm/^{144}Nd$, and 0.005% for $^{143}Nd/^{144}Nd$. Rb–Sr isotope analyses of samples 420/32 and 418/56 were performed at the Institute of the Earth's Crust, Irkutsk (M.N. Maslovskaya, analyst). Isotopic compositions in samples 427/2 and 420/54 are adopted from [7]. The multielement analysis of samples was carried out by the ICP-MS method on a PlasmaQuad 3 mass spectrometer (VG Elemental Company). Silicate analyses were performed at the Vinogradov Institute of Geochemistry and the Institute of the Earth's Crust, Irkutsk. Fe_2O_3 in the first four columns corresponds to the total Fe content. Oxides are given in wt %; elements, in ppm.

Thus, the data obtained do not contradict the concept of the genetic relation of the Vilyui paleorift system with the impact of a huge mantle plume upon the lithosphere. Centers of magmatic activity shifted from the south to the north in the course of evolution of the rift system. The initial stage of magmatism was marked by local centers of eruption in the southwestern part of the study region. Such eruptions gave way to large-scale magmatism in the entire rift region. The latest stage of magmatism was characterized by the formation of kimberlite pipes and postkimberlite dikes at the northwestern offshoots of the rift system.

ACKNOWLEDGMENTS

This work was supported by the Russian Foundation for Basic Research, project nos. 05-05-64043, 05-05-64000, and 06-05-64841.

REFERENCES

1. V. L. Masaitis, M. V. Mikhailov, and T. V. Selivanovskaya, *Volcanism and Tectonics of the Patom-Vilyui Aulacogene* (Nedra, Moscow, 1975) [in Russian].
2. V. V. Gaiduk, *The Vilyui Middle Paleozoic Rift System* (YaF SO AN SSSR, Yakutsk, 1988) [in Russian].
3. L. P. Zonenshain, M. I. Kuz'min, and L. M. Natapov, *Tectonics of Lithospheric plates in the USSR Territory* (Nedra, Moscow, 1990) [in Russian].
4. D. H. Abbott and A. E. Isley, J. Geol. **34**, 265 (2005).
5. R. E. Ernst and K. L. Buchan, Am. Geophys. Union. Geophys. Monogr. **100**, 297 (1997).
6. A. I. Kiselev, V. V. Yarmolyuk, K. N. Egorov, et al., Dokl. Earth Sci. **396**, 641 (2004) [Dokl. Akad. Nauk **396**, 660 (2004)].
7. A. I. Kiselev, V. V. Yarmolyuk, K. N. Egorov, et al., Petrology, No. 6, 588 (2006) [Petrologiya, No. 6, 680 (2006)].
8. S. S. Sun and W. F. McDonough, Geol. Soc. Am. Spec. Pap., No. 42, 313 (1989).
9. B. L. Weaver, Earth Planet. Sci. Lett. **104**, 381 (1991).